Macrophage Integrins Modulate Response to Ultra-High Molecular Weight Polyethylene Particles and Direct Particle-Induced Osteolysis

Toral D. Zaveri[1,3], **Natalia V. Dolgova**[1], **Jamal S. Lewis**[1,4], **Kiri Hamaker**[1], **Michael J. Clare-Salzler**[2], and **Benjamin G. Keselowsky**[1,*]

[1]J. Crayton Pruitt Family Department of Biomedical Engineering, University of Florida, Gainesville FL 32611 U.S

[2]Department of Pathology, Immunology and Laboratory Medicine, University of Florida, Gainesville FL 32611 U.S

[3]Department of Food Science, The Pennsylvania State University, University Park, PA 16802 U.S

[4]Department of Biomedical Engineering, University of California, Davis, Davis CA 95618

Abstract

Aseptic loosening due to peri-prosthetic osteolysis is one of the primary causes for failure of artificial joint replacements. Implant-derived wear particles, often ultra-high molecular weight polyethylene (UHMWPE) microparticles, initiate an inflammatory cascade upon phagocytosis by macrophages, which leads to osteoclast recruitment and activation, ultimately resulting in osteolysis. Investigation into integrin receptors, involved in cellular interactions with biomaterial-adsorbed adhesive proteins, is of interest to understand and modulate inflammatory processes. In this work, we investigate the role of macrophage integrins Mac-1 and RGD-binding integrins in response to UHMWPE wear particles. Using integrin knockout mice as well as integrin blocking techniques, reduction in macrophage phagocytosis and inflammatory cytokine secretion is demonstrated when these receptors are either absent or blocked. Along this line, various opsonizing proteins are shown to differentially modulate microparticle uptake and macrophage secretion of inflammatory cytokines. Furthermore, using a calvarial osteolysis model it is demonstrated that both Mac-1 integrin and RGD-binding integrins modulate the particle induced osteolysis response to UHMWPE microparticles, with a 40% decrease in the area of osteolysis by the absence or blocking of these integrins, *in vivo*. Altogether, these findings indicate Mac-1 and RGD-binding integrins are involved in macrophage-directed inflammatory responses to UHMWPE and may serve as therapeutic targets to mitigate wear particle induced peri-prosthetic osteolysis for improved performance of implanted joints.

---

*Corresponding Author: Benjamin G. Keselowsky, Tel: (352) 273-5878; Fax: (352) 392-9791; bgk@ufl.edu. Address: J. Crayton Pruitt Family Department of Biomedical Engineering, PO Box 116131, Gainesville, Florida, 32611-6131, USA.

Introduction

Aseptic loosening due to peri-implant osteolysis is one of the major reasons for failure of artificial joint implants [1], often requiring revision surgery [2]. This osteolysis results from osteoclast activation by macrophages that phagocytose wear debris particles generated during mechanical loading of the artificial joints [3]. The majority of hip joints that are replaced in the US have a metallic femoral stem and a metal or ceramic ball articulating with an ultra-high molecular weight polyethylene (UHMWPE) acetabular cup liner [4, 5]. Resulting wear-induced debris consists of particles derived from the various components of the implant including UHMWPE, bone cement in the form of poly(methyl methacrylate), or metal, with a predominant proportion of it being UHMWPE particles [4, 5]. Immediately following exposure to physiologic fluids, synthetic materials spontaneously adsorb a layer of host proteins which serves as a mediating layer between the debris particles and the immune cells recruited to the implant site. Macrophages form the majority of these recruited cells and play a significant role in the various phases of the foreign body response [6]. Macrophages, upon phagocytosing wear particles become activated and release prostaglandins, cytokines, metalloproteinases and lysosomal enzymes (e.g. TNF-α, IL-1β, IL-6, and PGE-2) which lead to activation of bone resorbing pathways [2, 7–9]. Considering the major role played by macrophages in the aseptic loosening process, several approaches have been investigated to mitigate the macrophage inflammatory response [10–13]. Although these approaches have shown some success in mitigating the inflammatory response, a clinical impact has yet to be realized.

Macrophages are phagocytes, one of the main professional antigen presenting cells of the body, and have been demonstrated to interact with wear particles *in vivo* [3, 14]. Macrophages interact with wear particles through the layer of adsorbed serum proteins including Type I collagen, aggrecan proteoglycans, immunoglobulin, fibronectin and albumin that have been identified on UHMWPE surfaces [15–17]. The type and amount of protein adsorbed on wear debris particles and the resulting bioreactivity in terms of the type of cytokines released also depends on the size [18] and material of the particle [15, 19, 20]. The interaction of adsorbed proteins and cell surface receptors, such as integrins, is known to be important for macrophage interactions with biomaterials [6, 21, 22]. Macrophage integrins direct numerous cell functions including phagocytosis of particulate matter, cell migration and spreading, paracrine signaling, and adhesion to extracellular matrix proteins as well as to other cells [23]. A critical clotting, and extracellular matrix protein, fibrinogen, mediates the acute inflammatory response by promoting phagocyte adhesion to foreign material following plasma deposition [24]. The integrin Mac-1 (CD11b/CD18) binds to fibrinogen and is present on macrophages, as well as neutrophils. Binding of Mac-1 to fibrinogen has been shown to direct macrophage adhesion and activation [25] and phagocytosis of titanium-alloy [26], polymethylmethacrylate [27] and stainless steel [28] microparticles. Considering the role Mac-1 plays in various inflammatory processes [29–31], it warrants further investigation in the context of modulating macrophage response to UHMWPE wear debris particles.

In addition to Mac-1, the role of other macrophage integrins is of interest, in particular, the RGD-binding integrins. The peptide sequence arginine-glycine-aspartic acid (RGD) was

first discovered in the protein fibronectin as the recognition site for the fibronectin receptor ($\alpha_5\beta_1$) [32]. It is also a known binding domain within numerous other proteins such as fibrinogen, vitronectin, von Willebrand factor, thrombospondin, laminin and collagen [33], all of which are proteins that can be found adsorbed onto biomaterial surfaces. The RGD sequence within these proteins can bind integrins abundantly present on the cell surface of macrophages, in particular, $\alpha_V\beta_3$, $\alpha_5\beta_1$ and $\alpha_V\beta_5$ [33], and can direct macrophage-biomaterial interactions. Hence, we are also interested in comparing the role RGD binding integrins, a broader class of integrins in the modulation of macrophage inflammatory responses.

In the present work, we uncover the role of integrin Mac-1 and RGD binding integrins in the macrophage response to UHMWPE microparticles (MPs). To investigate the role of the Mac-1 integrin in macrophage responses to particulate biomaterials, we quantify the phagocytosis of UHMWPE MPs and subsequent inflammatory cytokine secretion of macrophages derived from Mac-1 knockout (KO) mice in comparison to macrophages from wild type (WT) control mice. Similar studies were performed to determine the role of RGD-binding integrins using blocking peptide. Furthermore, we investigate the role of these integrins in *in vivo* particle-induced osteolysis using an established mouse calvarial model [34–36]. Elucidation of receptors mediating the inflammatory response to particles could drive the development of integrin-targeting therapeutic strategies to remedy peri-implant osteolysis.

Materials and Methods

Macrophage Generation

Bone marrow-derived macrophages were generated from 7–10 week-old C57BL6/J mice (wild type, WT) and B6.129S4-Itgam^{tm1Myd}/J mice (Mac-1 KO) using a 10-day culture protocol [31, 37–39]. Animals were handled in accordance with a protocol approved by the Institutional Animal Care and Use Committee (IACUC) at the University of Florida. Briefly, mice were euthanized by CO_2 asphyxiation followed by cervical dislocation and tibias and femurs were harvested for isolating marrow cells. Marrow cells were obtained by flushing the shaft of the bones with a 25 G needle using wash media comprised of RPMI media (Hyclone Laboratories Inc, Logan, Utah), 1% fetal bovine serum (FBS) (Hyclone Laboratories Inc, Logan, Utah) and 1% penicillin-streptomycin-neomycin antibiotic mixture (Hyclone Laboratories Inc, Logan, Utah). The macrophages were cultured in a growth media comprised of Dulbecco's Modified Eagle's Medium (DMEM)/F12 (1:1) (Cellgro, Herndon, VA) medium containing 1% penicillin-streptomycin, 1% L-glutamine (Lonza, Walkersville, MD), 1% non-essential amino acids (Lonza, Walkersville, MD), 1% sodium pyruvate (Lonza, Walkersville, MD), 10% fetal bovine serum (FBS) and 10% L-929 cell conditioned media (LCCM) (preparation described below). The LCCM serves as an established source of macrophage colony stimulating factor, which pushes the differentiation of marrow cells towards the macrophage phenotype [40]. From the isolated marrow cells, the red blood cells were lysed using ACK (Ammonium-Chloride-Potassium) lysis buffer (Lonza, Walkersville, MD). The precursor cells were isolated using centrifugation, resuspended in macrophage growth medium and then seeded in a tissue culture treated T-flask (day 0) to remove

fibroblasts and mature macrophages (adherent cell types). After 48 h (day 2), the floating cells were collected, resuspended in fresh media and seeded on low attachment plates for 4 additional days. The cells in the low attachment plates were supplemented with 1 ng/mL IL-3 (Peprotech, Rocky Hill, NJ) for expansion of the macrophage precursor cells. Half of the media in the low attachment wells was exchanged on day 4 with fresh growth media. At the end of 6 days, cells were lifted from the low attachment wells by gentle pipetting, re-suspended and seeded on tissue culture-treated polystyrene plates for 2 more days to allow macrophage adhesion and maturation. On day 8, all the media in the wells was replaced with fresh media and at day 10 of culture, the cells were ready for experiment. A high purity (~87%) population of macrophages was obtained at the end of the 10 day culture protocol which was verified by staining for CD11b (α chain of Mac-1) and F4/80 murine macrophage markers and analyzed using flow cytometry [39]. Macrophages isolated from at least 4 separate mice were used for each type of experiment.

LCCM Preparation

To produce LCCM, L-929 cells were grown to a confluent monolayer in 150 cm^2 tissue culture flasks. 50 mL media was added to each flask for 7 days after which all the media in the flask was replaced with fresh media for 7 additional days. The media collected at day 7 and 14 was pooled, sterile-filtered and stored at $-20°C$.

Microparticle Preparation for *in vitro* Studies

UHMWPE particles (made available from Shamrock Technologies, Newark, NJ) in the size range of 0.5–5 μm were used to model wear debris particles generated *in vivo*. Macrophage inflammatory response to wear particles has been shown to depend on the size and shape of the wear particles with particles in the size range of 0.5–5 eliciting a strong inflammatory response [41, 42].

In order to visualize and quantify the number of UHMWPE MPs phagocytosed by the macrophages, the opsonizing proteins used to coat the particles were fluorescently labeled using Alexa Fluor® succinimidyl ester fluorescent dyes. The different proteins used for opsonization were human plasma-derived fibronectin (FN) (BD Bioscience) and bovine plasma fibrinogen (Fg) (MP Biomedicals) as well as FBS and Bovine serum albumin (BSA) (Fisher Bioreagents). For protein conjugation the Alexa Fluor® dye was mixed with protein solutions of FN, Fg and BSA (5 mg/mL) according to the desired labeling efficiency and allowed to react by stirring for one hour at room temperature. After one hour, the unreacted dye was separated from the protein solution by centrifugation through spin filters with a pore size of 3 kDa. The particles were vortexed into the labeled protein solution (250 μg/mL) and allowed to incubate with the protein overnight at 4°C. After overnight incubation, the particles were separated from labeled protein solution by filtration (pore size 0.22 μm) and resuspended by sonication into respective unlabeled protein solutions (250 μg/mL) to prepare an aggregate-free stock solution. The stock concentration of the fluorescent MPs was determined by quantifying fluorescent events using the Guava® EasyCyte® 8HT flow cytometer, which is microfluidics-based and does not utilize diluting sheath fluid to provide particle counting data.

Analysis of endotoxin on MPs was performed with the chromolimulus amoebocyte lysate (Chromo-LAL) assay [31] (Associates of Cape Cod Incorporated, Falmouth, MA). Briefly, 50 μL of the Chromo-LAL substrate (LimulusAmebocyte Lysate co-lyophilized with chromogenic substrate) was mixed with 50 μL of endotoxin-free water containing protein coated MPs (20 million/ml) in a 96-well plate. The 96-well plate was then read in a microplate reader measuring absorbance at 405 nm every 2 min for 2 h at room temperature. Based on the manufacturer's instructions, a threshold absorbance value of 0.2 was selected and the time point that the sample crossed the threshold value was used for calculating the endotoxin concentration with the help of a standard curve plotted with the control standard endotoxin provided by the manufacturer. The detection limit of the assay at 2 h is 0.04 EU/mL.

For cytokine quantification following phagocytosis, the MPs were not fluorescently labeled and were prepared differently. According to previously published studies by our group as well as others, a detectable level of endotoxin on MPs of specific materials has been reported to be a prerequisite for inflammatory cytokine secretion [31, 43–46]. Hence MPs coated with known level of endotoxin were prepared for the cytokine study. In order to remove adherent endotoxin on the UHMWPE MPs, they were washed in 70% ethanol for 72 hours by continuous shaking and ethanol change every 24 hours. The endotoxin levels on the particles cleaned using this procedure was quantified and determined to be below detectable limits (0.005 EU/mL). To coat the clean MPs with a known amount of endotoxin, particles were incubated with 100% ethanol containing 3–5 μg/mL (depending on the protein to be adsorbed later) lipopolysaccharide (LPS) for 1 hour. The different proteins with different sizes and binding affinity for the MP surface necessitated different LPS concentration to ensure comparable endotoxin values (5 EU/million MPs-ml) on MPs irrespective of protein coating. The clean MPs to be used as endotoxin free controls were also incubated in 100% ethanol without LPS. After 1 hour, the MPs are separated from ethanol by spin filtration (pore size 0.22 μm) and resuspended in solutions of FN, Fg and BSA (250 μg/mL) or Serum (5% in Phosphate-buffered saline (PBS)). MPs with and without LPS coating were incubated with protein solutions for 2 hours after which the endotoxin levels on the MPs was measured [31].

The size distribution of the particles with different adsorbed proteins was determined using LS13 320 laser diffraction particle size analyzers ((Beckman Coulter) PERC, University of Florida) and using a number percent-based calculation to ensure different opsonizing proteins do not change the size distribution of MPs due to aggregation. Cumulative percentages within different size ranges was then calculated. The size and surface properties of MPs were also visualized and corroborated using JEOL SEM-6400 Scanning Electron Microscopy (SEM). (MAIC facility, University of Florida).

In vitro Quantification of Macrophage Phagocytosis of Polyethylene Microparticles

For *in vitro* phagocytosis experiments, macrophages (1×10^5/well) were plated to confluence at 16 h of seeding in 96 well tissue culture plates. Fluorescently labeled protein-coated UHMWPE MPs were added to each well at either 20:1 or 40:1 MP:cell ratio. The density of UHMWPE is 0.94g/cm^3, which is lower than water (1g/cm^3) hence when

suspended in media, the MPs float to the surface and do not make contact with macrophages adherent on the bottom of the well. To ensure microparticle contact with the cells, wells were filled to the brim with macrophage media, sealed with a sealing tape, inverted and incubated at 37°C, 5% CO_2. MP uptake was evaluated at the end of 2, 3.5, 5 and 7.5 hours after two PBS washes to remove non-phagocytosed MPs and read in a fluorescent plate reader. The number of MPs phagocytosed was determined from a standard curve obtained by plotting relative fluorescence intensity versus MP number. The results are reported as MPs/cell and normalized for cell numbers by staining cell nuclei with DAPI, a DNA staining dye and measuring fluorescence intensity per well [31].

Inverted Cell Culture and Macrophage Cytokine Production *in vitro*

Because UHMWPE density is less than water, MPs float on the surface of the cell culture media, presenting a challenge to a conventional experimental set-up. A number of studies have used various techniques to confine MPs to the bottom of well plates such as agarose embedding, but which have the disadvantage of limiting the macrophage interactions with embedded microparticles [47]. We have therefore implemented an inverted culture system comprising of macrophages cultured on glass coverslips inverted over Viton O rings which keep the coverslip at a set height from the bottom of the well (Figure 1), as previously reported [39]. The UHMWPE MPs float to the top of the media, which is adjusted to be at the level of the coverslip allowing free interaction between the cells and MPs. The Viton O rings were prepared for cell culture experiments by sterilization in an autoclave.

For quantification of Mac-1 KO and WT macrophage cytokine production, macrophages (1×10^6/coverslip) were grown to confluence at 16 h of seeding on 22×22 mm glass coverslips (Fisherbrand, Fisher Scientific). Protein coated MPs with or without adsorbed LPS were added to each well in order to get a MP:cell ratio of 10:1. The well plates are incubated at 37°C, 5% CO2 for 24 hours to allow phagocytosis and secretion of cytokines. Untreated cells were setup as a negative control for the baseline cytokine secretion, whilst an additional control of cells incubated with 1 μg/mL soluble LPS was the positive control due to activation by a strong inflammatory signal. After 24 h, the supernatant was collected and frozen at −20°C for cytokine analysis using sandwich ELISA [48, 49]. The supernatant was assayed for cytokines TNF-α and IL-6 using sandwich ELISA kits (R&D Systems) according to the manufacturer's directions.

For RGD blocking experiments, macrophages (1×10^5/well) plated in 96 well tissue culture plates were incubated with 10 mM RGD in macrophage media for 1 h prior to adding microparticles. MPs coated with the opsonizing protein fibronectin were added at a MP:cell ratio of 10:1, the plate was sealed with sealing tape, inverted and macrophages were maintained in contact with microparticles for 24h to allow cytokine secretion. After 24 h, the supernatant was collected and frozen at −20°C for quantifying TNF-α and IL-6 secretion using sandwich ELISA.

Disc Preparation for Controlled Release of RGD *In Vivo*

To deliver RGD peptide to the site of MP implantation *in vivo* we used the controlled release system, ethylene vinyl acetate (EVA) polymer, a non-inflammatory and non-biodegradable

polymer that has been investigated for slow and sustained release of compounds into the brain [50] as well as tooth space [51]. EVA was loaded with RGD peptide by the emulsion-solvent evaporation method [31, 52–54]. Briefly, a 10% (w/v) solution of the EVA polymer was prepared by dissolving it in methylene chloride. Polymer/drug solution was prepared by mixing the EVA polymer solution and RGD peptide dissolved in PBS (10mg in 50 μL) in a ratio of 6.5:3.5 (v/v) in sealed glass vessels. This solution was agitated vigorously for 15 min followed by sonication in a water bath at 25°C for 15 min. Each film sample was prepared using 35 μL of the resulting dispersion and placing a drop on a treated glass coverslip, followed by quick-freezing on dry ice and then dried under vacuum to remove any solvent by evaporation. The coverslip was sprayed with hydrophobic coating of Rain-X™ to allow easy peeling of the film from the coverslip surface. The resulting films were approximately 7 mm in diameter and 0.2 mm in thickness. Control discs were prepared similarly using the EVA polymer without loading the RGD peptide.

Loading efficiency of the RGD peptide in the EVA polymer was determined by dissolving the prepared discs back into methylene chloride followed by addition of PBS to extract the peptide in the aqueous phase. This emulsion was agitated vigorously for 15 min followed by sonication in a water bath at 25°C for 15 min. The emulsion was then centrifuged at $10,000 \times g$ for 10 min to allow separation of the oil and water phase of the emulsion. The aqueous phase was collected, and analyzed using spectrophotometric techniques to determine the RGD concentration, and therefore the peptide loading for each disc. More specifically, the concentration of RGD peptide was calculated by measuring absorbance at 280 nm and comparing that value to known concentrations from a standard curve plotted using RGD solutions with known concentrations.

Release kinetics of the encapsulated RGD peptide from the EVA discs, were characterized over 3 weeks with continuous shaking in PBS (pH=7.4) at 37°C. The discs were placed on a shaker and the supernatant was collected and replenished with fresh PBS every 3 days. Using spectrophotometric analysis as described above, the concentration of RGD peptide in the supernatant was determined and the release was plotted as a percentage of loaded RGD released over 3 weeks.

Mouse Calvarial Osteolysis Model

To investigate the role of different integrins in wear particle-induced osteolysis *in vivo*, we used an established mouse calvarial osteolysis model [34–36]. UHMWPE microparticles were implanted directly on the surface of the calvarial bone and the extent of osteolysis was quantified using histomorphometry. Briefly, mice were anesthetized with 70–80 mg/kg ketamine and 5–7 mg/kg xylazine following protocols approved by the UF IACUC. The head of the mouse was shaved and the calvaria were exposed with a one centimeter incision in the frontal plane between the two ears. 6 mg of UHMWPE MPs in 30 μL of 0.1% FBS was spread on the calvarial surface over the periosteum and the incision was closed using 7 mm stainless steel wound clips. Care was taken to clip the wound clips in with the prongs into the skin and not facing skull. Wild type mice designate as "sham" had the calvaria exposed and wound clips applied without particles implanted on the calvarium to determine the osteolysis resulting from surgery alone. Wild type mice designated as "vehicle"

underwent surgery with 30 μL of 0.1% FBS without particles implanted on the calvarium to determine the effect of the solution used to suspend the UHMWPE MPs. The numbers of mice in each group are shown in Table 1. For the Mac-1 integrin study, the resulting osteolysis from the implanted particles was quantified in Mac-1 KO mice and compared to WT controls. For the RGD integrin study, additional controls of vehicle + blank EVA disc and MPs with Blank EVA disc were included using WT mice, to study the additional inflammation resulting from the EVA disc. Differences in the area of osteolysis between the control groups, vehicle only and vehicle only + blank EVA, were not significant. As such, these groups were combined under the vehicle control label. Additionally, the area of osteolysis for the wild type MPs only group and the MPs + blank EVA disc were not statistically different and were combined under the WT MPs label.

Seven days post-surgery, mice were euthanized by CO_2 asphyxiation, and the calvaria removed for histological processing. Briefly, the calvaria were fixed in 10% formalin and decalcified using 10% Ethylenediaminetetraacetic acid (EDTA) at 4°C for 7 days, which enabled paraffin embedding and sectioning. Five micron sections of the paraffin embedded calvaria were taken in the frontal plane around the area where the MPs were placed. The sections were stained with hemotoxylin and eosin for nuclei (dark blue) and protein, typically primarily collagen (pink) and imaged using phase-contrast microscopy (Axiovert 200M Carl Zeiss inverted fluorescent microscope). The cross sectional area of proteinaceous soft tissue 1.5 mm around the midline suture was measured via image analysis as indicative of the area of bone resorption. Independent histomorphometry measurements on subsets of each of experimental group were performed by a separate grader, yielding an inter-grader correlation of $R^2 = 0.78$.

Statistical Analysis

Statistical analyses were performed using general linear nested model ANOVA, using Systat (Version 12, Systat Software, Inc., San Jose, CA). Pair-wise comparisons between Mac-1 KO and WT groups for the *in vitro* studies were made using student's t-test to determine significant differences. Comparison between the different opsonizing proteins for the Mac-1 KO *in vitro* studies, and between experimental groups in the *in vitro* RGD blocking studies, as well as *in vivo* studies were made using Tukey's Honestly-Significant-Difference Test with p-values of less than or equal to 0.05 considered to be significant.

Results

Purity of macrophage culture

In order to verify generation of a relatively pure macrophage population from the bone marrow precursor cells, at the end of the 10 d culture protocol, cells were incubated with fluorescently labeled antibodies against CD11b and F480, murine macrophage markers. The number of cells expressing these markers was quantified using flow cytometry. Approximately, 90% of the cells from the WT mice stained for both the macrophage markers indicating a high purity macrophage population (Figure 2A). Using the same method, the number of macrophages expressing CD11b (Mac-1) in the Mac-1 KO mice was also quantified. Approximately 99% of the F4/80 macrophages from the Mac-1 KO mice did

not express CD11b, thus there was an effective knockdown of the Mac-1 (CD11b) receptor (Figure 2B).

UHMWPE Microparticle Characterization

Opsonizing proteins were used (fibrinogen - Fg, fibronectin - FN, Serum, and bovine serum albumin - BSA) to coat ultra-high molecular weight polyethylene (UHMWPE) microparticles (MPs). Morphology and size distribution of UHMWPE MPs was determined by scanning electron microscopy and dynamic light scattering (Figure 3). A representative scanning electron microscopic image of the UHMWPE MPs depicts the characteristic irregular shape and rough surface texture of these particles (Figure 3A). In terms of size distributions, over 90% of the MPs coated with fibronectin, fibrinogen and serum were in the size range of 0.5–5 μm, with ~35% in the submicron size range (Figure 3B), which has been suggested to be most reactive in terms of cytokine secretion [41, 42]. In contrast, the BSA coated MPs demonstrated some agglomeration with a small shift towards a larger size distribution; with less than 10% MPs in the submicron size range and higher percentage of MPs greater than 5 μm.

Role of Mac-1 Integrins in Microparticle Uptake *in vitro*

The role of Mac-1 in macrophage MP uptake was quantified using UHMWPE MPs coated with opsonizing proteins (BSA, Fg, FN) at different time points (2 h, 3.5 h, 5 h, 7.5 h) (Figure 4). Note that while washing steps were utilized to separate unbound MPs from cells, measurements in the experimental design utilized do not distinguish between internalized and the more tightly surface-bound MPs which resist removal. Results indicate both the opsonizing protein and receptor group (Mac-1 KO versus wild type; WT) were found to simultaneously influence MP uptake, as indicated by the ANOVA interaction term p-value ($p<0.05$). Wild type macrophages differentially phagocytosed MPs depending on which opsonizing protein was used. In particular, higher uptake levels were measured for Fg-coated MPs and lower uptake of BSA coated MPs for all time points tested except for 3.5 h, at which time uptake of FN-coated MPs was equivalent to Fg-coated MPs. It is noted that the fewer BSA coated MPs phagocytosed by macrophages compared to Fg coated MPs may be at least partially a result of the modest agglomeration seen for the BSA coated MPs, where MP size is a known determinant of uptake [55, 56].

The absence of Mac-1 resulted in a 20–50% decrease in uptake of opsonized MPs compared to WT control, with an average reduction of 30%, in the majority of cases. Against this trend, Mac-1 KO and WT macrophages phagocytosed an equivalent of FN-opsonized MPs at 5 h, and Fg-opsonized MPs at 7.5 h, and surprisingly, a greater number of FN-opsonized MPs at 7.5 h. It is possible compensatory mechanisms in the Mac-1 KO macrophages, such as up-regulation of other integrins that bind to fibronectin, may be engaged at these points.

Role of Mac-1 and RGD Integrins in Macrophage Inflammatory Cytokine Secretion in Response to UHMWPE MPs *in vitro*

The roles of both opsonizing proteins and integrin receptors in inflammatory cytokine production upon UHMWPE MP uptake was next investigated (Figure 5). In order to determine the role of Mac-1, comparisons were made between Mac-1 KO macrophages and

WT macrophages, whereas RGD-blocking peptide was utilized to assess the role of RGD-binding integrins. Of note, the 72 h ethanol wash protocol used for removal of endotoxin (see Methods section) produced clean, endotoxin-free UHMWPE MPs. These endotoxin-free MPs were unable to induce inflammatory cytokine responses in macrophages at detectable amounts, consistent with reports from us and other groups [31, 43–45]. Therefore, as a model system to mimic MP-induced inflammation in macrophages, clean MPs were incubated with a defined amount of activating lipopolysaccharide (LPS; a prototypical endotoxin) followed by opsonizing proteins. The LPS coating concentration was adjusted to provide an equivalent adsorbed LPS amount for all protein coatings. Pre-coated MPs were then incubated with macrophages and cytokines present in the supernatant were quantified after 24 h. Comparing across opsonin groups, Fg and FN demonstrated lower levels of secreted IL-6 than the Serum and BSA coated MPs (Figure 5A). Similarly for TNF-α secretion, Serum, Fg, and FN coated MPs had lower levels compared to BSA for WT macrophages (Figure 5B). For Mac-1 KO macrophages, TNF-α levels were lower for Serum and Fg opsonized MPs compared to BSA, with FN at an intermediate level. Untreated control macrophages for both WT and KO demonstrated undetectable levels of both IL-6 and TNF-α.

Regarding the role of Mac-1 in an IL-6 response to MP uptake, Mac-1 KO macrophages demonstrated a modest 15% reduction compared to WT when the opsonin was BSA (Figure 5A). In contrast, Fg, FN and Serum opsonized MPs yielded no differences in IL-6 secretion. Regarding TNF-α secretion, Mac-1 KO macrophages also demonstrated a modest 10–20% reduction compared to WT for Fg, Serum and BSA opsonized MPs (Figure 5B). Interestingly, there was also a 10–15% decrease in both TNF-α and IL-6 levels by Mac-1 KO macrophages when incubated with soluble LPS (included as a positive control). This finding is consistent with the report that Mac-1 is integral, in coordination with CD-14 and TLR-4 receptors, for signal transduction in response to LPS, and consistent with our previous finding using polystyrene MPs [31, 57]. This suggests Mac-1 plays a role in cytokine responses to both soluble LPS, and LPS-adsorbed, protein-opsonized UHMWPE MPs.

The use of soluble blocking RGD peptide to inhibit integrin binding to surface adsorbed adhesive proteins has been well established [31, 58]. Blocking concentrations of soluble RGD peptide to macrophage cultures was next utilized to investigate the role of RGD-binding integrins in macrophage inflammatory cytokine responses (Figure 6). In this instance, after LPS pre-coating, FN was selected to opsonize UHMWPE MPs, representing the quintessential RGD containing adhesive protein. Secretion of IL-6 and TNF-α upon phagocytosis of MPs was then quantified at 24 h. Remarkably, a large decrease in both cytokines was evident upon RGD blocking. Specifically, IL-6 decreased 70% in the RGD blocked group (Figure 6A), and TNF-α decreased even more, at ~90% compared to unblocked control (Figure 6B). Notably, these cytokine levels were comparable to the base line level of macrophages without the addition of MPs. This indicates a large role for RGD-binding integrins in cytokine responses to these opsonized UHMWPE MPs.

Role of Mac-1 Integrins in Particle-Induced Osteolysis *in vivo*

In order to investigate the role of Mac-1 integrin in particle-induced osteolysis, the area of resulting osteolysis was quantified *in vivo* following implantation of UHMWPE MPs onto Mac-1 KO or WT mouse calvaria (Figure 7A). No pre-coating of MPs was required, as UHMWPE readily adsorbs opsonins *in vivo*. Control groups consisting of a sham surgery (no implant), vehicle (0.1% serum used to suspend the UHMWPE MPs) were included for comparison. Mean and standard error of pooled results were plotted and analyzed by ANOVA (Figure 7A). Notably, the area of osteolysis induced by UHMWPE MPs in the Mac-1 KO mouse was ~40% lower than the WT control, and at a comparable level to that of the vehicle only, indicating a considerable role for Mac-1 integrin. Additionally, no difference between the sham and the vehicle was detected, indicating that the 0.1% FBS vehicle used to suspend the MPs did not contribute to the osteolytic process. Representative hematoxylin and eosin stained sections of the mouse calvaria from each group are shown (Figure 8A–D), with arrows pointing to representative areas of proteinaceous tissue, indicating osteolysis. These data indicate Mac-1 integrin is significantly involved in the osteolytic response to UHMWPE MPs.

Role of RGD-binding Integrins in Particle-Induced Osteolysis *in vivo*

In order to provide extended delivery of RGD blocking peptide to the site of MP implantation *in vivo*, peptide was incorporated into an ethylene vinyl acetate (EVA) polymer film. Ethylene vinyl acetate is a non-inflammatory and non-biodegradable polymer that has been investigated for slow and sustained release of compounds in numerous anatomical locations such as the brain [50] and tooth space [51]. The loading efficiency of RGD into the EVA disc was determined to be 92%, providing 2.3 mg of encapsulated RGD peptide per disc. The *in vitro* release characteristic of RGD from the disc was determined over the course of 3 weeks (Figure 9). A linear early release of RGD from the discs was measured in the first four days, releasing ~50% of the encapsulated peptide. This was followed by a gradual increase to ~65% of the encapsulated peptide in the next 4 days followed by a plateau phase, with negligible release for the next 2 weeks of testing. This release profile was deemed adequate for the 7 d *in vivo* MP-induced osteolysis experiment.

To next investigate role of RGD-binding integrins, the area of osteolysis resulting from implanted UHMWPE MPs with and without inclusion of RGD peptide in EVA polymer discs was determined (Figure 7B). Control groups consisting of a sham surgery (no implant), vehicle only (0.1% serum used to suspend the UHMWPE MPs) and a vehicle + blank EVA (no RGD peptide loaded) group were also included for comparison against the experimental group (MPs + RGD Block). Mean and standard error of pooled results were plotted and analyzed by ANOVA (Figure 7B). Of primary interest, the area of osteolysis in the RGD-blocking group was 40% lower than in the mice with the blank EVA discs. As above, the RGD-blocked samples were at comparable level to that of the sham and vehicle controls, indicating a major role for RGD-binding integrins as well. Additionally, the two control groups sham and vehicle were not significantly different, indicating that the 0.1% FBS vehicle used to suspend the MPs did not contribute to the osteolytic process. Representative sections of the mouse calvaria from each group are shown (Figure 8A, B, D, E) depicting the

example areas of osteolysis (arrows). These data indicate RGD binding integrins are also significantly involved in the osteolytic response to UHMWPE MPs.

Discussion

Macrophage response to MPs generated from friction in artificial joints is the initial event in the process of aseptic loosening [7]. Microparticles settle in the spaces between the implant shaft and the bone, where they are phagocytosed by macrophages, which become activated giving rise to an inflammatory response [7]. Macrophage activation upon binding to the proteins adsorbed on biomaterial surfaces, results in the release of inflammatory cytokines such as TNF-α, IL-6, IL-1 and prostaglandin-E all of which are known to activate osteoclastic pathways [2, 8, 9]. Hence targeting the process at this early stage may be a valuable point of mitigation, thus reducing the incidence of aseptic loosening and the need for revision surgeries for artificial joints.

Using UHMWPE particles to model the peri-prosthetic wear debris generated in the body, we investigated the role of macrophage integrins Mac-1 and RGD-binding integrins in the particle uptake, subsequent cytokine secretion and resulting osteolysis *in vivo*. Notably, there are contradicting reports in the field regarding the necessity of adsorbed endotoxin for an inflammatory response to wear particles. Some groups have reported a macrophage inflammatory cytokine response with undetectable levels of endotoxin [47, 49], whereas others have demonstrated the lack of inflammatory response in the absence of detectable endotoxin levels on MPs [43–45]. However, careful attention is required as to the endotoxin quantification methods employed, and reports often do not provided sufficient information regarding the endotoxin quantification procedure used [59, 60]. Because the chromo-LAL endotoxin assay is sensitive to the number of particles tested, and the volume in which they are tested, it is not possible to interpret studies where these values are not reported. Additionally, because endotoxin adhered to microparticle surfaces, studies that test only the supernatants without the actual particles likely produce erroneous results [45]. Furthermore, chromo-LAL is a kinetic assay and quantification can depend on the endpoint selected by the user from a range specified by the manufacturer. Hence a detailed description of the endotoxin quantification is necessary to allow standardized comparisons. Consistent with our prior study using polystyrene microparticles [31], in the present investigation, we found that while UHMWPE MP uptake is not affected by adsorbed endotoxin, endotoxin-free MPs result in undetectable levels of *in vitro* macrophage cytokine secretion. Therefore, as an *in vitro* model system producing an inflammatory macrophage response, a normalized amount (5 EU/million MPs-ml) of MP-adsorbed LPS was utilized.

On the other hand, *in vivo* studies with well-documented endotoxin-free microparticles have been shown to induce osteolysis. Our results are consistent with this. For the *in vivo* calvarial osteolysis study, we utilized endotoxin free UHMWPE MPs, and demonstrate particle-induced osteolysis. One potential reason endotoxin-free particles are capable of inducing osteolysis may result from adsorption from systemic endotoxin derived from minor infections, or intestinal or dental flora [61]. Another proposed *in vivo* mechanism of immune activation by orthopedic wear particles is the chemical modification of the surface of particles, as shown by Maitra et al., which demonstrated oxidation of implanted

polyethylene as a mechanism for immune recognition and activation. They demonstrated *in vitro* activation of dendritic cells (upregulation of MHC-II and IL-12 secretion) when incubated with retrieved polyethylene from implant revision surgeries and hydroxyl-or carboxyl-modified polyethylene, but not with unmodified polyethylene [62]. Overall, given the complexity, it is important to note interpretation of the present results are confined to the specific conditions investigated.

Based on the results of the MP uptake studies with Mac-1 KO macrophages, Mac-1 plays a role in MP uptake. The reduced uptake by Mac-1 KO macrophages compared to WT macrophages is particularly evident at earlier time points for all opsonins. This indicates a role for Mac-1 in ligand-specific kinetics of receptor-mediated macrophage phagocytosis. The substantial downstream effects seen with the decrease in IL-6 and TNF-α cytokine secretion corroborate this. For MPs opsonized with Fg and BSA, Mac-1 KO macrophages showed reduced MP uptake as well as reduced secretion of cytokines TNF-α. UHMWPE MPs are extremely hydrophobic and it has been shown that proteins such as fibrinogen and albumin that adsorb onto such hydrophobic surfaces such as UHMWPE undergo extensive denaturation/unfolding [21, 22, 63]. For example, Fg adopts an energetically favorable unfolded conformation thereby exposing the hidden epitopes P1 (γ 190–202) and P2 (γ 377–395), which are known to be binding sites for integrin Mac-1. Mac-1 is known to bind to denatured proteins [64] which may explain the reduced particle uptake and cytokine secretion for protein opsonized MPs, especially fibrinogen and albumin, by Mac-1 KO macrophages. Fibronectin, a known ligand for integrin Mac-1 [65], when adsorbed on MPs also showed reduced uptake by Mac-1 KO macrophages at early time points, however this relationship reversed with time. Macrophage adhesion to fibronectin is shown to be mediated by other β_1, β_3, and β_5 integrins[66], which may be upregulated in absence of Mac-1 leading to increased MP uptake in Mac-1 KO compared to WT controls at later time points. Interestingly, the positive control, soluble LPS group resulted in lower IL-6 and TNF-α levels from Mac-1 KO macrophages, compared to WT. This observation is in agreement with work done by Vogel et al., where they found that integrin Mac-1 complexes with the CD-14 receptor [67], and TLR-4 in response to LPS, and that the complex is required for expression of the whole spectrum of inflammatory genes [68]. Supporting this, LPS-induced NF-kB translocation and MAPK activation has been shown to be downregulated in Mac-1 deficient mice [57].

To delineate the role of Mac-1 integrins in the peri-prosthetic osteolysis process, we quantified the in vivo osteolysis resulting from implanting polyethylene microparticles on the surface of mouse calvaria, which was shown to be 40% lower in Mac-1 KO mice. This finding is consistent with the *in vitro* results characterizing reduced MP uptake and inflammatory cytokine secretion by macrophages. Previously, the integrin Mac-1 has been shown to mediate macrophage adhesion to adsorbed proteins and direct phagocytosis of titanium-alloy wear particles [26]. Our finding on MP uptake and cytokine secretion studies with Mac-1 KO macrophages extend the observation of this effect to UHMWPE MPs for both *in vitro* and *in vivo* settings.

Notably, the role of Mac-1 integrin in the osteolysis process may be at least twofold; first through the modulation of macrophage response to wear particles and second through its

role in osteoclasts maturation and activation, which complicates interpretation. Osteoclast precursors undergoing differentiation to osteoclasts have a macrophage like phenotype and express macrophage receptors such as Mac-1 and Mac-2 [69]. It has also been reported that blocking the Mac-1 receptor using antibodies against CD11b (α_M) and CD18 (β_2) subunits results in inhibition of osteoclast differentiation in both RAW264.7 cells and bone marrow derived macrophages upon addition of RANKL [70]. Thus the absence of Mac-1 integrin impairs osteoclast differentiation directly through the absence of a required receptor Mac-1 as well indirectly through decreased activating cytokines.

Integrin $\alpha_V\beta_3$ is important for inflammatory responses in activated macrophages [71]. Blocking macrophage integrin receptors with RGD-binding activity such as $\alpha_V\beta_3$, $\alpha_5\beta_1$ and $\alpha_V\beta_5$ with soluble RGD peptide, has previously been shown to prevent uptake of protein coated polystyrene MPs, as well as subsequent inflammatory cytokine secretion [31]. To investigate the role of RGD binding integrins in the *in vivo* particle-induced osteolysis response, osteolysis was quantified in the presence or absence of RGD blocking peptide by the controlled release of peptide via co-implanted RGD loaded EVA polymer discs, and quantification demonstrated 40% lower osteolysis in mice with the RGD blocking peptide. This result is consistent with the *in vitro* RGD blocking results characterizing reduced inflammatory cytokine secretion by macrophages in response to UHMWPE MPs.

Similar to the role of integrin Mac-1 in the osteolysis process, the role of RGD-binding integrin is also two-fold; through reduced MP uptake and cytokine secretion as well as the possibility of altered osteoclast activation due to receptor blocking. Multiple integrins present on osteoclasts such as $\alpha_V\beta_3$, $\alpha_2\beta_1$ and $\alpha_V\beta_1$ [72] are known to bind to the RGD domain in proteins. Osteoclasts actively migrate on the surface of bone and undergo alternating cycles of migration and resorption [73]. Both of these processes involve interaction with extracellular matrix which occurs through integrins, and integrins are thus key players in the osteoclast resorption process [74]. For example, RGD blocking peptide binding to the integrin receptors is known to disrupt osteoclast-extracellular matrix interaction, preventing binding of osteoclasts to bone surface and prevents formation of a sealing zone which is required for the resorption process [75].

Thus, we have identified that both Mac-1 and RGD-binding integrins play a role in the *in vitro* macrophage inflammatory responses and the *in vivo* osteolytic response to UHMWPE MPs. Targeting Mac-1 and RGD-binding integrins may serve as therapeutic foci to mitigate peri-implant osteolysis.

Acknowledgments

Reference list

1. Callaghan, JJ., Rosenberg, AG., Rubash, HE. The adult hip. Lippincott Williams & Wilkins; 2007.

2. Bauer TW, Schils J. The pathology of total joint arthroplasty. II. Mechanisms of implant failure. Skeletal radiology. 1999; 28:483–97. [PubMed: 10525792]

3. Amstutz, HC., Campbell, P., Kossovsky, N., Clarke, IC. Clinical orthopaedics and related research. 1992. Mechanism and clinical significance of wear debris-induced osteolysis; p. 7-18.

4. Doorn PF, Campbell PA, Amstutz HC. Metal versus polyethylene wear particles in total hip replacements. A review. Clinical orthopaedics and related research. 1996:S206–16. [PubMed: 8769335]

5. Wooley PH, Schwarz EM. Aseptic loosening. Gene therapy. 2004; 11:402–7. [PubMed: 14724679]

6. Anderson JM. Biological responses to materials. Annual Review of Materials Research. 2001; 31:81–110.

7. Ingham E, Fisher J. The role of macrophages in osteolysis of total joint replacement. Biomaterials. 2005; 26:1271–86. [PubMed: 15475057]

8. Merkel KD, Erdmann JM, McHugh KP, Abu-Amer Y, Ross FP, Teitelbaum SL. Tumor necrosis factor-alpha mediates orthopedic implant osteolysis. The American journal of pathology. 1999; 154:203–10. [PubMed: 9916934]

9. Yokohama Y, Matsumoto T, Hirakawa M, Kuroki Y, Fujimoto N, Imai K, et al. Production of matrix metalloproteinases at the bone-implant interface in loose total hip replacements. Laboratory investigation; a journal of technical methods and pathology. 1995; 73:899–911. [PubMed: 8558853]

10. Childs LM, Goater JJ, O'Keefe RJ, Schwarz EM. Efficacy of etanercept for wear debris-induced osteolysis. Journal of bone and mineral research: the official journal of the American Society for Bone and Mineral Research. 2001; 16:338–47.

11. Trindade MC, Lind M, Nakashima Y, Sun D, Goodman SB, Schurman DJ, et al. Interleukin-10 inhibits polymethylmethacrylate particle induced interleukin-6 and tumor necrosis factor-alpha release by human monocyte/macrophages in vitro. Biomaterials. 2001; 22:2067–73. [PubMed: 11432585]

12. Loi F, Córdova LA, Zhang R, Pajarinen J, Lin T-h, Goodman SB, et al. The effects of immunomodulation by macrophage subsets on osteogenesis in vitro. Stem Cell Research & Therapy. 2016; 7:1–11. [PubMed: 26729060]

13. Goodman SB, Gibon E, Pajarinen J, Lin TH, Keeney M, Ren PG, et al. Novel biological strategies for treatment of wear particle-induced periprosthetic osteolysis of orthopaedic implants for joint replacement. Journal of the Royal Society Interface. 2014; 11:20130962.

14. Tuan RS, Lee FY, YTK, Wilkinson JM, Smith RL. Implant Wear Symposium Biologic Work G. What are the local and systemic biologic reactions and mediators to wear debris, and what host factors determine or modulate the biologic response to wear particles? J Am Acad Orthop Surg. 2008; 16(Suppl 1):S42–8. [PubMed: 18612013]

15. Bosetti M, Zanardi L, Bracco P, Costa L, Cannas M. In vitro evaluation of the inflammatory activity of ultra-high molecular weight polyethylene. Biomaterials. 2003; 24:1419–26. [PubMed: 12527283]

16. Wooley PH, Fitzgerald RH, Song Z, Davis P, Whalen JD, Trumble S, et al. Proteins Bound to Polyethylene Components in Patients Who Have Aseptic Loosening After Total Joint Arthroplasty. A Preliminary Report*. The Journal of Bone & Joint Surgery. 1999; 81:616–23. [PubMed: 10360690]

17. Zolotarevova E, Hudecek J, Spundova M, Entlicher G. Binding of proteins to ultra high molecular weight polyethylene wear particles as a possible mechanism of macrophage and lymphocyte activation. Journal of biomedical materials research Part A. 2010; 95:950–5. [PubMed: 20845495]

18. Reddy A, Caicedo M, Samelko L, Jacobs JJ, Hallab NJ. Implant debris particle size affects serum protein adsorption which may contribute to particle size-based bioreactivity differences. Journal of long-term effects of medical implants. 2014; 24:77–88. [PubMed: 24941408]

19. Maloney WJ, Sun DH, Nakashima Y, James R, Smith RL. Effects of serum protein opsonization on cytokine release by titanium-alloy particles. Journal of biomedical materials research. 1998; 41:371–6. [PubMed: 9659605]

20. Sun D-H, Trindade MCD, Nakashima Y, Maloney WJ, Goodman SB, Schurman DJ, et al. Human serum opsonization of orthopedic biomaterial particles: Protein-binding and monocyte/

macrophage activation in vitro. Journal of Biomedical Materials Research Part A. 2003; 65A:290–8.

21. Flick MJ, Du X, Degen JL. Fibrin(ogen)-alpha M beta 2 interactions regulate leukocyte function and innate immunity in vivo. Experimental biology and medicine. 2004; 229:1105–10. [PubMed: 15564436]

22. Ratner BD, Bryant SJ. Biomaterials: where we have been and where we are going. Annual review of biomedical engineering. 2004; 6:41–75.

23. Gordon, S. The macrophage as therapeutic target. Springer; 2003.

24. Tang L, Eaton JW. Fibrin(ogen) mediates acute inflammatory responses to biomaterials. The Journal of experimental medicine. 1993; 178:2147–56. [PubMed: 8245787]

25. Altieri DC, Mannucci PM, Capitanio AM. Binding of fibrinogen to human monocytes. The Journal of clinical investigation. 1986; 78:968–76. [PubMed: 3760194]

26. Nakashima Y, Sun DH, Trindade MC, Maloney WJ, Goodman SB, Schurman DJ, et al. Signaling pathways for tumor necrosis factor-alpha and interleukin-6 expression in human macrophages exposed to titanium-alloy particulate debris in vitro. The Journal of bone and joint surgery American volume. 1999; 81:603–15. [PubMed: 10360689]

27. Rakshit DS, Lim JTE, Ly K, Ivashkiv LB, Nestor BJ, Sculco TP, et al. Involvement of complement receptor 3 (CR3) and scavenger receptor in macrophage responses to wear debris. Journal of Orthopaedic Research. 2006; 24:2036–44. [PubMed: 16947312]

28. Baldwin L, Flanagan BF, Hunt JA. Flow cytometric measurement of phagocytosis reveals a role for C3b in metal particle uptake by phagocytes. Journal of Biomedical Materials Research Part A. 2005; 73A:80–5.

29. Coxon A, Rieu P, Barkalow FJ, Askari S, Sharpe AH, von Andrian UH, et al. A novel role for the beta 2 integrin CD11b/CD18 in neutrophil apoptosis: a homeostatic mechanism in inflammation. Immunity. 1996; 5:653–66. [PubMed: 8986723]

30. Ehlers MR. CR3: a general purpose adhesion-recognition receptor essential for innate immunity. Microbes and infection/Institut Pasteur. 2000; 2:289–94.

31. Zaveri TD, Lewis JS, Dolgova NV, Clare-Salzler MJ, Keselowsky BG. Integrin-directed modulation of macrophage responses to biomaterials. Biomaterials. 2014; 35:3504–15. [PubMed: 24462356]

32. Pierschbacher MD, Ruoslahti E. Cell attachment activity of fibronectin can be duplicated by small synthetic fragments of the molecule. Nature. 1984; 309:30–3. [PubMed: 6325925]

33. Ruoslahti E. RGD and other recognition sequences for integrins. Annual review of cell and developmental biology. 1996; 12:697–715.

34. Schwarz EM, Lu AP, Goater JJ, Benz EB, Kollias G, Rosier RN, et al. Tumor necrosis factor-alpha/nuclear transcription factor-kappaB signaling in periprosthetic osteolysis. Journal of orthopaedic research: official publication of the Orthopaedic Research Society. 2000; 18:472–80. [PubMed: 10937636]

35. Taki N, Tatro JM, Nalepka JL, Togawa D, Goldberg VM, Rimnac CM, et al. Polyethylene and titanium particles induce osteolysis by similar, lymphocyte-independent, mechanisms. Journal of orthopaedic research: official publication of the Orthopaedic Research Society. 2005; 23:376–83. [PubMed: 15734251]

36. von Knoch M, Jewison DE, Sibonga JD, Sprecher C, Morrey BF, Loer F, et al. The effectiveness of polyethylene versus titanium particles in inducing osteolysis in vivo. Journal of orthopaedic research: official publication of the Orthopaedic Research Society. 2004; 22:237–43. [PubMed: 15013080]

37. Cunnick J, Kaur P, Cho Y, Groffen J, Heisterkamp N. Use of bone marrow-derived macrophages to model murine innate immune responses. Journal of immunological methods. 2006; 311:96–105. [PubMed: 16563426]

38. Stanley, ER. Murine Bone Marrow-Derived Macrophages. In: Pollard, J., Walker, J., editors. Basic Cell Culture Protocols. Humana Press; 1997. p. 301-4.

39. Zaveri TD, Dolgova NV, Chu BH, Lee J, Wong J, Lele TP, et al. Contributions of surface topography and cytotoxicity to the macrophage response to zinc oxide nanorods. Biomaterials. 2010; 31:2999–3007. [PubMed: 20074795]

40. Tomida M, Yamamoto-Yamaguchi Y, Hozumi M. Purification of a factor inducing differentiation of mouse myeloid leukemic M1 cells from conditioned medium of mouse fibroblast L929 cells. The Journal of biological chemistry. 1984; 259:10978–82. [PubMed: 6469994]

41. Green TR, Fisher J, Matthews JB, Stone MH, Ingham E. Effect of size and dose on bone resorption activity of macrophages by in vitro clinically relevant ultra high molecular weight polyethylene particles. Journal of biomedical materials research. 2000; 53:490–7. [PubMed: 10984696]

42. Shanbhag AS, Jacobs JJ, Black J, Galante JO, Glant TT. Macrophage/particle interactions: effect of size, composition and surface area. Journal of biomedical materials research. 1994; 28:81–90. [PubMed: 8126033]

43. Bi Y, Seabold JM, Kaar SG, Ragab AA, Goldberg VM, Anderson JM, et al. Adherent endotoxin on orthopedic wear particles stimulates cytokine production and osteoclast differentiation. Journal of bone and mineral research: the official journal of the American Society for Bone and Mineral Research. 2001; 16:2082–91.

44. Daniels AU, Barnes FH, Charlebois SJ, Smith RA. Macrophage cytokine response to particles and lipopolysaccharide in vitro. Journal of biomedical materials research. 2000; 49:469–78. [PubMed: 10602080]

45. Ragab AA, Van De Motter R, Lavish SA, Goldberg VM, Ninomiya JT, Carlin CR, et al. Measurement and removal of adherent endotoxin from titanium particles and implant surfaces. Journal of orthopaedic research: official publication of the Orthopaedic Research Society. 1999; 17:803–9. [PubMed: 10632445]

46. Alley C, Haggard W, Smith R. Effect of UHMWPE Particle Size, Dose, and Endotoxin on in vitro Macrophage Response. 2014; 24:45–56.

47. Ingram JH, Stone M, Fisher J, Ingham E. The influence of molecular weight, crosslinking and counterface roughness on TNF-alpha production by macrophages in response to ultra high molecular weight polyethylene particles. Biomaterials. 2004; 25:3511–22. [PubMed: 15020125]

48. Hallab NJ, McAllister K, Brady M, Jarman-Smith M. Macrophage reactivity to different polymers demonstrates particle size- and material-specific reactivity: PEEK-OPTIMA® particles versus UHMWPE particles in the submicron, micron, and 10 micron size ranges. Journal of Biomedical Materials Research Part B: Applied Biomaterials. 2012; 100B:480–92.

49. Matthews JB, Green TR, Stone MH, Wroblewski BM, Fisher J, Ingham E. Comparison of the response of three human monocytic cell lines to challenge with polyethylene particles of known size and dose. Journal of materials science Materials in medicine. 2001; 12:249–58. [PubMed: 15348309]

50. Bix GJ, Clark GD. Elvax as a slow-release delivery agent for a platelet-activating factor receptor agonist and antagonist. Journal of neuroscience methods. 1997; 77:67–74. [PubMed: 9402559]

51. Dolce C, Vakani A, Archer L, Morris-Wiman JA, Holliday LS. Effects of echistatin and an RGD peptide on orthodontic tooth movement. Journal of dental research. 2003; 82:682–6. [PubMed: 12939350]

52. Lewis JS, Dolgova NV, Zhang Y, Xia CQ, Wasserfall CH, Atkinson MA, et al. A combination dual-sized microparticle system modulates dendritic cells and prevents type 1 diabetes in prediabetic NOD mice. Clin Immunol. 2015; 160:90–102. [PubMed: 25842187]

53. Lewis JS, Roche C, Zhang Y, Brusko TM, Wasserfall CH, Atkinson M, et al. Combinatorial delivery of immunosuppressive factors to dendritic cells using dual-sized microspheres. J Mater Chem B Mater Biol Med. 2014; 2:2562–74. [PubMed: 24778809]

54. Lewis JS, Zaveri TD, Crooks CP 2nd, Keselowsky BG. Microparticle surface modifications targeting dendritic cells for non-activating applications. Biomaterials. 2012; 33:7221–32. [PubMed: 22796161]

55. Champion JA, Walker A, Mitragotri S. Role of Particle Size in Phagocytosis of Polymeric Microspheres. Pharmaceutical research. 2008; 25:1815–21. [PubMed: 18373181]

56. Pacheco P, White D, Sulchek T. Effects of Microparticle Size and Fc Density on Macrophage Phagocytosis. PLoS ONE. 2013; 8:e60989. [PubMed: 23630577]

57. Perera PY, Mayadas TN, Takeuchi O, Akira S, Zaks-Zilberman M, Goyert SM, et al. CD11b/CD18 acts in concert with CD14 and Toll-like receptor (TLR) 4 to elicit full lipopolysaccharide and taxol-inducible gene expression. Journal of immunology. 2001; 166:574–81.

58. Garcia AJ, Schwarzbauer JE, Boettiger D. Distinct activation states of alpha5beta1 integrin show differential binding to RGD and synergy domains of fibronectin. Biochemistry. 2002; 41:9063–9. [PubMed: 12119020]

59. Pajarinen J, Mackiewicz Z, Pollanen R, Takagi M, Epstein NJ, Ma T, et al. Titanium particles modulate expression of Toll-like receptor proteins. Journal of biomedical materials research Part A. 2010; 92:1528–37. [PubMed: 19425045]

60. Pearl JI, Ma T, Irani AR, Huang Z, Robinson WH, Smith RL, et al. Role of the Toll-like receptor pathway in the recognition of orthopedic implant wear-debris particles. Biomaterials. 2011; 32:5535–42. [PubMed: 21592562]

61. Tatro JM, Taki N, Islam AS, Goldberg VM, Rimnac CM, Doerschuk CM, et al. The balance between endotoxin accumulation and clearance during particle-induced osteolysis in murine calvaria. Journal of orthopaedic research: official publication of the Orthopaedic Research Society. 2007; 25:361–9. [PubMed: 17106883]

62. Maitra R, Clement CC, Crisi GM, Cobelli N, Santambrogio L. Immunogenecity of Modified Alkane Polymers Is Mediated through TLR1/2 Activation. PLoS ONE. 2008; 3:e2438. [PubMed: 18560588]

63. Wang J, Chen X, Clarke ML, Chen Z. Vibrational Spectroscopic Studies on Fibrinogen Adsorption at Polystyrene/Protein Solution Interfaces: Hydrophobic Side Chain and Secondary Structure Changes. The Journal of Physical Chemistry B. 2006; 110:5017–24. [PubMed: 16526745]

64. Davis GE. The Mac-1 and p150,95 beta 2 integrins bind denatured proteins to mediate leukocyte cell-substrate adhesion. Experimental cell research. 1992; 200:242–52. [PubMed: 1572393]

65. Lishko VK, Yakubenko VP, Ugarova TP. The interplay between integrins alphaMbeta2 and alpha5beta1 during cell migration to fibronectin. Experimental cell research. 2003; 283:116–26. [PubMed: 12565824]

66. Roach T, Slater S, Koval M, White L, McFarland EC, Okumura M, et al. CD45 regulates Src family member kinase activity associated with macrophage integrin-mediated adhesion. Current Biology. 1997; 7:408–17. [PubMed: 9197241]

67. Lee JD, Kravchenko V, Kirkland TN, Han J, Mackman N, Moriarty A, et al. Glycosyl-phosphatidylinositol-anchored or integral membrane forms of CD14 mediate identical cellular responses to endotoxin. Proceedings of the National Academy of Sciences of the United States of America. 1993; 90:9930–4. [PubMed: 7694296]

68. Vogel S, Hirschfeld MJ, Perera PY. Signal integration in lipopolysaccharide (LPS)-stimulated murine macrophages. Journal of endotoxin research. 2001; 7:237–41. [PubMed: 11581577]

69. Tsurukai T, Takahashi N, Jimi E, Nakamura I, Udagawa N, Nogimori K, et al. Isolation and characterization of osteoclast precursors that differentiate into osteoclasts on calvarial cells within a short period of time. Journal of Cellular Physiology. 1998; 177:26–35. [PubMed: 9731742]

70. Hayashi H, Nakahama K, Sato T, Tuchiya T, Asakawa Y, Maemura T, et al. The role of Mac-1 (CD11b/CD18) in osteoclast differentiation induced by receptor activator of nuclear factor-kappaB ligand. FEBS letters. 2008; 582:3243–8. [PubMed: 18775427]

71. Wilder RL. Integrin alpha V beta 3 as a target for treatment of rheumatoid arthritis and related rheumatic diseases. Annals of the rheumatic diseases. 2002; 61(Suppl 2):ii96–9. [PubMed: 12379637]

72. Clover J, Dodds RA, Gowen M. Integrin subunit expression by human osteoblasts and osteoclasts in situ and in culture. Journal of cell science. 1992; 103(Pt 1):267–71. [PubMed: 1429908]

73. Kanehisa J, Heersche JN. Osteoclastic bone resorption: in vitro analysis of the rate of resorption and migration of individual osteoclasts. Bone. 1988; 9:73–9. [PubMed: 3044405]

74. Duong LT, Lakkakorpi P, Nakamura I, Rodan GA. Integrins and signaling in osteoclast function. Matrix biology: journal of the International Society for Matrix Biology. 2000; 19:97–105. [PubMed: 10842093]

75. Engleman VW, Nickols GA, Ross FP, Horton MA, Griggs DW, Settle SL, et al. A peptidomimetic antagonist of the alpha(v)beta3 integrin inhibits bone resorption in vitro and prevents osteoporosis in vivo. The Journal of clinical investigation. 1997; 99:2284–92. [PubMed: 9151803]
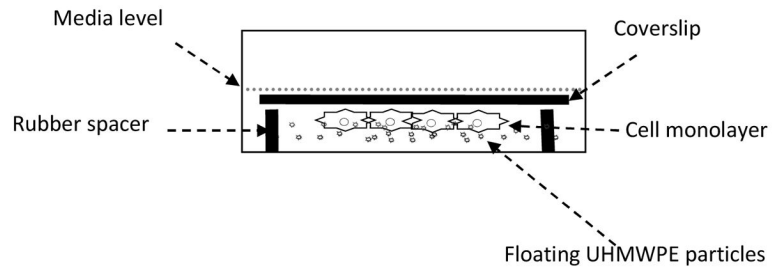
Figure 1.
Details of a single well for inverted culture phagocytosis assay. The UHMWPE particles float in media, and contact macrophages cultured on inverted coverslips. Coverslips are placed onto Viton O-rings as a spacer. The setup facilitates the free interaction and close contact between macrophages and UHMWPE particles.
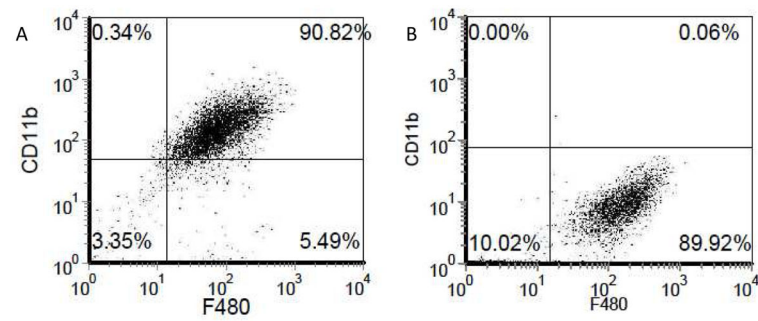
Figure 2.
A) Purity of the macrophage culture was determined to be ~90% by immunofluorescent quantification of F4/80 and CD11b, murine macrophage markers B) The deficiency of Mac-1 receptor on macrophages from the Mac-1 KO mouse was verified by staining for CD11b (α chain of Mac-1). The percentage of cells expressing CD11b was determined to be ~1%.
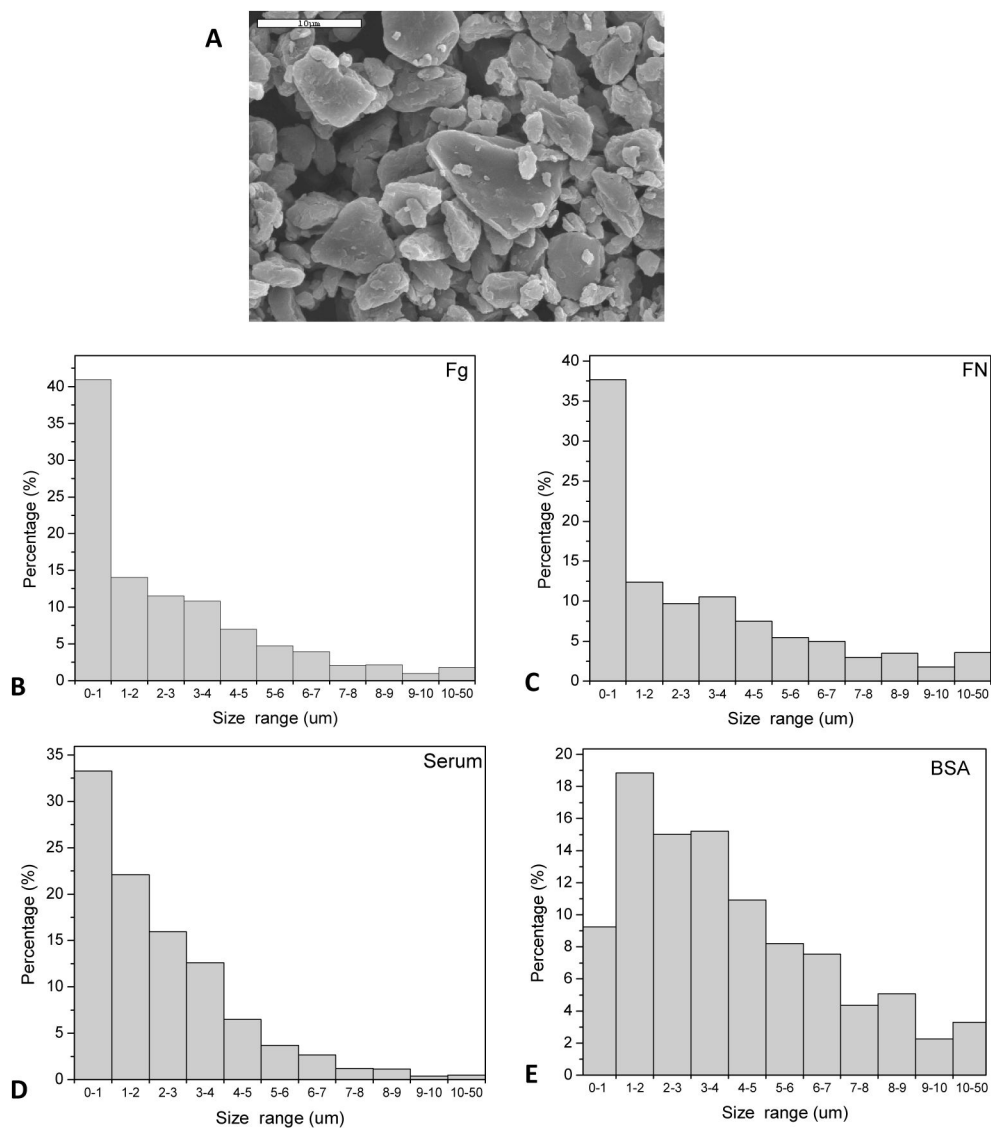
Figure 3.
Particle size distribution of protein coated UHMWPE microparticles. A) SEM image of BSA coated UHMWPE microparticles (scale bar = 10 μm) showing the size distribution, shape and surface texture of the UHMWPE microparticles. Microparticles coated with B) Fg C) FN D) Serum and E) BSA were analyzed for size distribution using laser diffraction particle size analyzer.
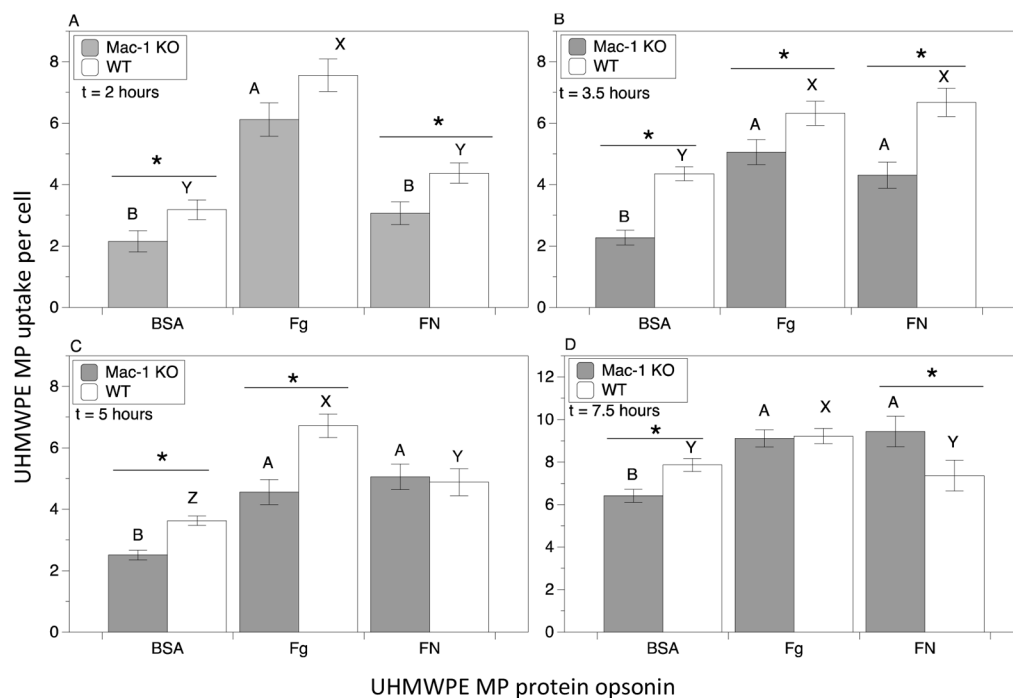
Figure 4.
Integrin Mac-1 modulates macrophage uptake of fluorescently labeled protein-opsonized UHMWPE microparticles (MPs). Microparticles pre-coated with opsonizing protein were incubated with macrophages at a 40:1 ratio of MP:cell, and uptake was quantified at: A.) 2 h B.) 3.5 h C.) 5 h, and D.) 7.5 h. Results comparing Mac-1 KO macrophages to WT controls as well comparing particle uptake across different opsonizing protein coatings within the same group (Mac-1 KO or WT) are shown. The average number of MPs per cell taken up was quantified by pooling data from at least 24 samples from 4 separate runs. Plotted are mean and standard error. Pair-wise significant differences using t-test between Mac-1 KO and WT control samples for each protein coating is denoted by the * symbol (p value < 0.05). Uppercase letters denote significant differences (p < 0.05) among all groups analyzed by ANOVA and Tukey's post hoc test, where groups labeled with a differing capital letters are significantly different from each other, and groups with identical capital letters are not.
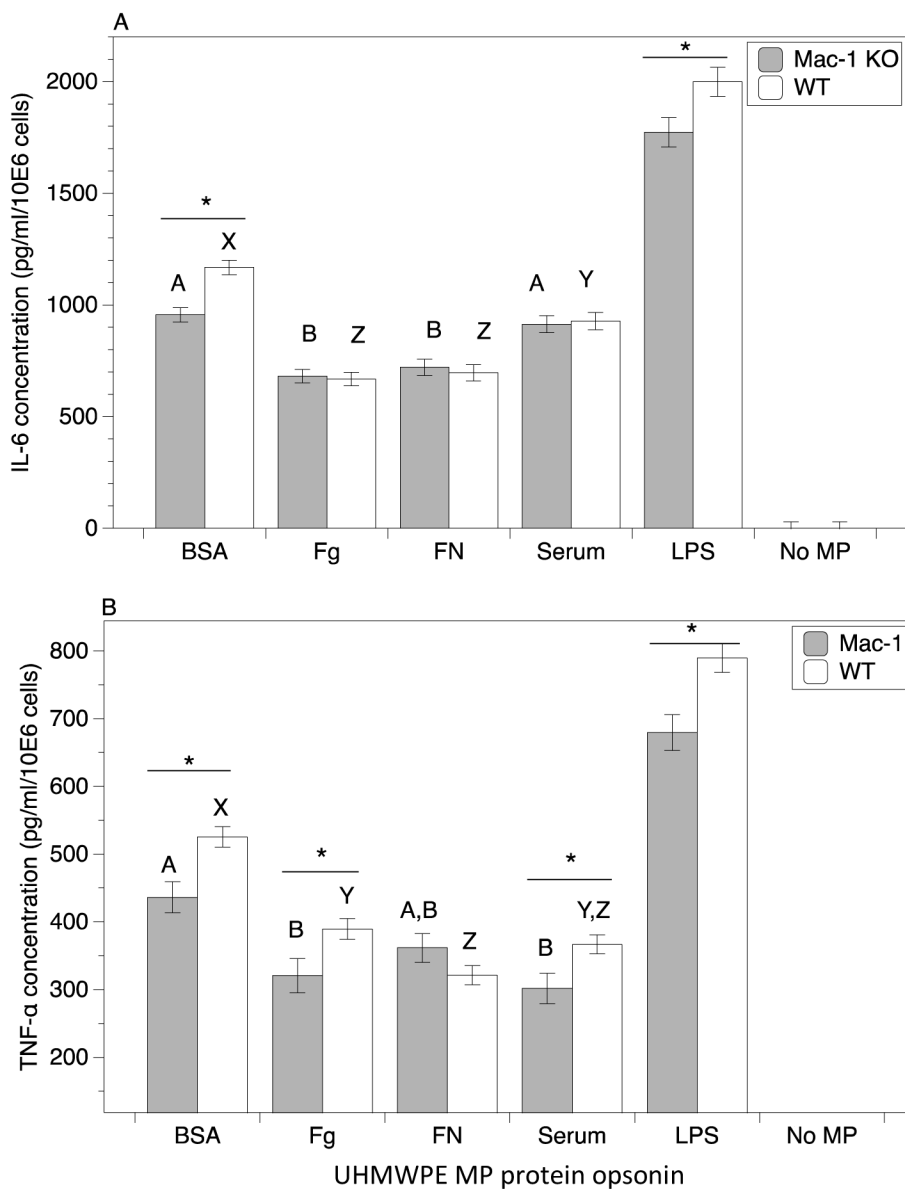
Figure 5.
Integrin Mac-1 modulates macrophage cytokine secretion in response to protein-opsonized, LPS-coated UHMWPE microparticles (MPs). Secreted cytokines: A.) IL-6, and B.) TNF-α, from Mac-1 KO and WT macrophages upon 24 h exposure to protein-opsonized, LPS-coated (5 EU/million MPs-mL) UHMWPE MPs. Cytokine concentrations were quantified by pooling data from 24 samples from 4 separate runs. Plotted are mean and standard error. Significant differences between Mac-1 KO and WT control samples using t-test for each protein coating is denoted by the * symbol (p value < 0.05). Uppercase letters denote significant differences (p < 0.05) among all groups analyzed by ANOVA and Tukey's post hoc test, where groups labeled with a differing capital letters are significantly different from each other, and groups with identical capital letters are not.
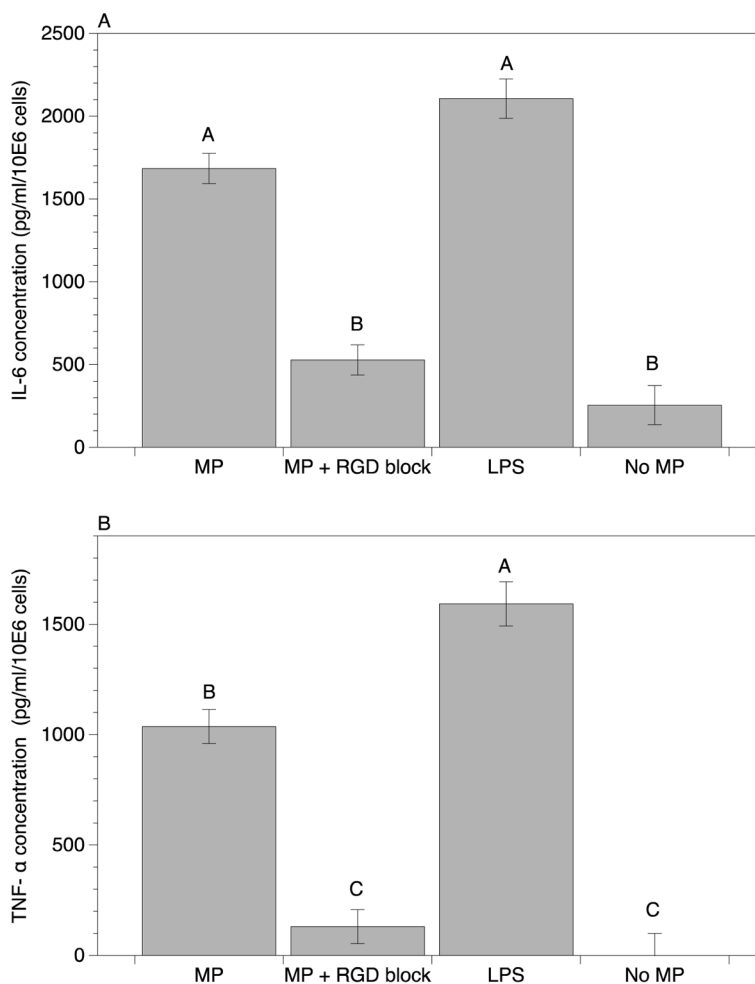
Figure 6.
Blocking RGD-binding integrins modulates macrophage cytokine secretion in response to fibronectin-opsonized, LPS-coated UHMWPE microparticles (MPs). Secreted cytokines: A.) IL-6, and B.) TNF-α, from macrophages in response to 24 h exposure to fibronectin-opsonized, LPS-coated (5 EU/million MPs-mL) MPs with or without RGD blocking with 10 mM soluble peptide. Positive control of soluble LPS (1μg/ml) and a negative control of macrophages cultured without MPs was included. Cytokine concentrations were quantified by pooling data from 6 samples from 2 separate runs. Plotted are mean and standard error. Uppercase letters denote significant differences (p < 0.05) among all groups analyzed by ANOVA and Tukey's post hoc test, where groups labeled with a differing capital letters are significantly different from each other, and groups with identical capital letters are not.
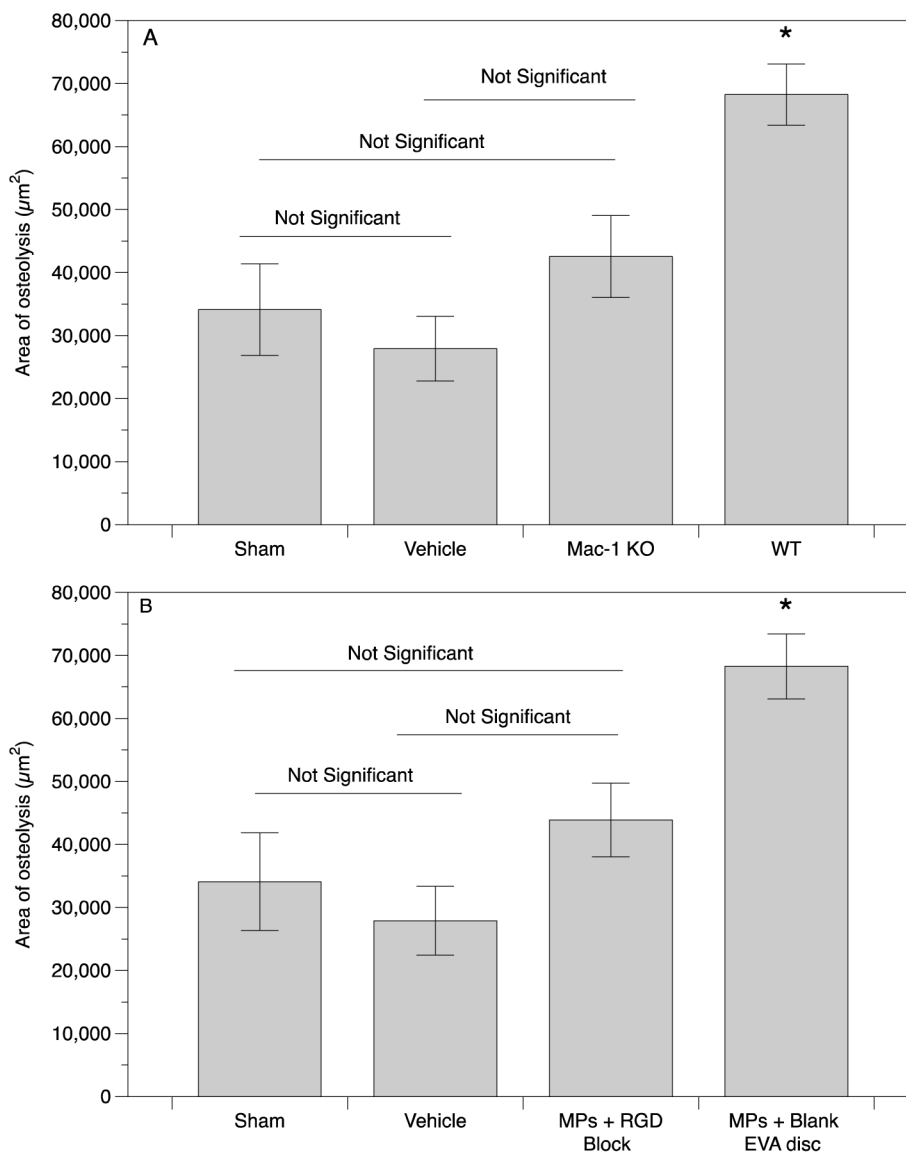
Figure 7.
A) Integrin Mac-1 modulates osteolysis in response to UHMWPE microparticles. B) RGD-binding integrins modulate osteolysis in response to UHMWPE microparticles. The area of osteolysis around the midline suture was quantified at 7 d. Average area of osteolysis was quantified by pooling data from 10 histological slices per mouse and number of mice per group are shown in Table 1. Plotted are mean and standard error. (* indicates statistically significant difference ($p < 0.05$) from all other groups.
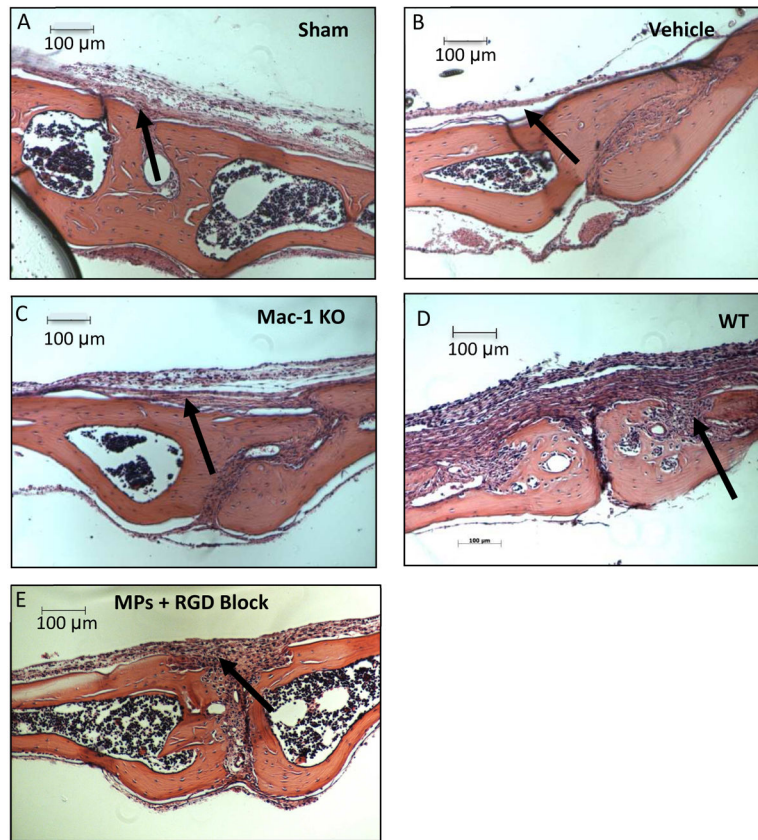
Figure 8.
Decalcified calvaria were sectioned and stained with hematoxylin and eosin for osteolysis measurement. Representative images of calvaria from A) Sham and B) Vehicle C) Mac-1 KO D) WT and E) WT + RGD loaded EVA disc are shown to depict the difference in area of osteolysis, with regions of osteolysis indicated (arrows).
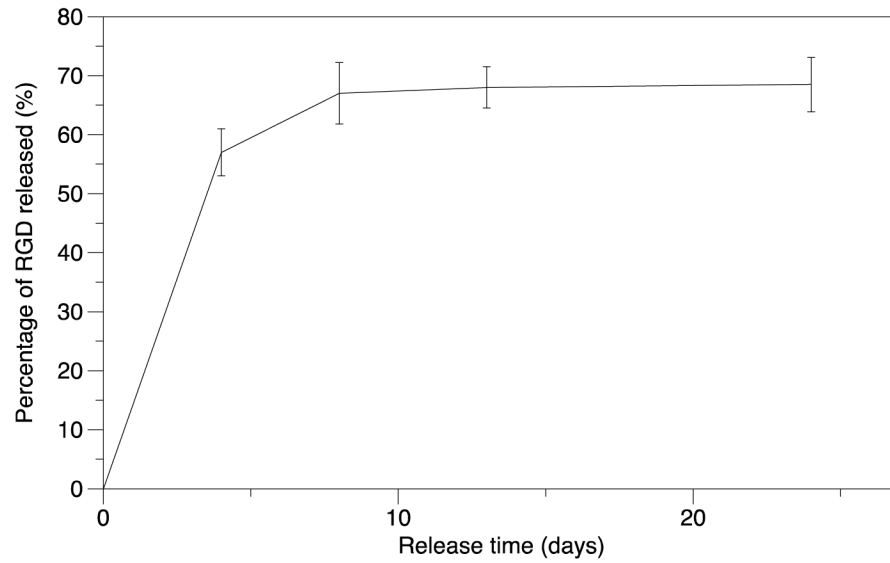
Figure 9.
Release kinetics of RGD peptide from EVA polymer films. Over 65% of the encapsulated peptide is released within 8 days. Each point represents the mean and standard deviation of 3 samples.

Table 1

Description of number of mice included within each experimental/control group for the calvarial osteolysis surgery

	Male	Female
WT Sham	4	0
WT Vehicle	4	0
WT Vehicle + Blank EVA disc	4	0
WT MPs + Blank EVA disc	2	1
WT MPs	6	0
WT MPs + RGD loaded EVA disc	6	1
Mac-1 KO MPs	4	1